Silk Fibroin Films Decorated with Magnetic Nanoparticles for Wound Healling Applications

MIHAELA CRISTINA BUNEA[1], EUGENIA VASILE[2], BIANCA GALATEANU[3], ARIANA HUDITA[3], MIRELA SERBAN[3], CATALIN ZAHARIA[1]*

[1] University Politehnica of Bucharest, Advanced Polymer Materials Group, 1-7 Gh. Polizu Str. Bucharest 011061, Romania

[2] University Politehnica of Bucharest, 313 Splaiul Independentei, 060042, Bucharest, Romania

[3] University of Bucharest, Department of Biochemistry and Molecular Biology, 91-95 Splaiul Independentei, 050095, Bucharest, Romania

The paper is focused on designing a novel silk fibroin-magnetite biomaterial scaffold for wounds healing in terms of: synthesis, physico-chemical and morphological characterization and in vitro biological behaviour assessment. Magnetic scaffolds were prepared from silk fibroin solutions and magnetic nanoparticles with various concentrations by solvent casting technique. Specimens were investigated by FTIR-ATR spectroscopy and XRD measurements. Morphological investigation including internal structure was employed by AFM and TEM/HRTEM analyses. Biological assay was performed on human adipose derived stem cells isolated from subcutaneous adipose tissue. Results suggested that all the tested magnetic silk-magnetite scaffolds display a good biocompatibility in vitro on hASCs and could be promising candidates for further wound dressing testing.

Keywords: silk fibroin, magnetite, wound dressing, scaffold

Silk fibroin is a natural fibrous protein produced by domesticated silkworm *Bombyx mori*, spiders or insects such as *Nephila clavipes* [1-5]. Silks are high molecular weight block copolymers consisting of a heavy (~370 kDa) and a light (~26 kDa) chain with varying amphiphilicity linked by a single disulfide bond [6-9]. These natural silkworm proteins have a highly repetitive amino acid sequence mainly composed of glycine (43%), alanine (31%), and serine (12%) residues [8-12]. The particular sequence of these amino acids with small side chains leads to the formation of hydrophobic domains, thus allowing the formation of thick packs of hydrogen bonded anti-parallel β-sheets [3,6-9]. Aqueous processing conditions, biocompatibility, good water vapour and oxygen permeability and biodegradability of silk fibroin, along with facile chemical modifications, are attractive features for its use as biomaterial. *Bombyx mori* mulberry silkworms are of the most economic importance, because it is possible to rear them in captivity. The fact that there is a readily available source of silkworm silk has facilitated an understanding of its structure and function.

Biomaterial design is an important element of tissue engineering, incorporating physical, chemical and biological cues to guide cells into functional tissues. Many biomaterials need to degrade at a rate commensurate with new tissue formation to allow cells to deposit new extracellular matrix (ECM) and regenerate functional tissue. In addition, biomaterials may need to include provisions for mechanical support appropriate to the level of functional tissue development.

Therefore, silks have been investigated as biomaterials due to the successful use of silk fibers from *Bombyx mori* as suture material for centuries [1, 12-14]. Its uses rely on the excellent mechanical properties in fibre state, on the possibilities of chemically modifying and processing the protein, lack of toxicity, lack of immune reactions, permeability to water vapours and oxygen [10-14]. The medical applications of natural silk fibroin, regenerated by dissolution and precipitation or chemically modified fibroin refer to the obtaining of suture fibres, materials for wound dressing, hydrogels based on fibroin for immobilization or controlled release of active principles, tissue reconstruction and cell culture etc.

Silk scaffolds have been thoroughly studied for potential biotechnological and biomedical applications. To improve the properties of scaffolds, silk fibroin has been blended with various other polymers, which includes synthetic polymers such as polyvinyl alcohol as well as natural macromolecules like gelatin, collagen, elastin, etc [15-19]. In a previous work [14] we have reported the synthesis and complex characterization of silk fibroin/ polyacrylamide hydrogels for tissue engineering applications. The use of silk fibroin as a scaffold for tissue engineering is a challenge for scientists all over the world.

Magnetite (Fe_3O_4) is a particular magnetic material and receiving special effort due to its potential applications in high-density data storage, biomaterial applications, catalysis, magnetic resonance imaging, Li-ion batteries, sensors, pigments and others [20-23]. With the rapid development of nanotechnology, magnetic nanoparticles are now being studied all over the world. In recent years, magnetic nanoparticles, especially magnetite has been used to develop a wide range of biomedical and bioengineering applications such as: magnetic resonance imaging, contrast agents, biosensors, cancer hyperthermia and targeted drug delivery [20-23]. Most of the envisaged applications are based on the unique magnetic properties of these nanoparticles, namely, their capacity to display high magnetization in the presence of an external magnetic field and insignificant residual magnetism in its absence. Nanosized magnetic carriers provide good performance due to their higher specific surface area and lower internal diffusion resistance. Based on a recent report, the presence of iron oxide in hydroxyapatite can improve the radiopacity and osteoblast proliferation [22]. Fe_3O_4 doped HA exhibits enhanced solubility in physiological solutions compared with HA [23]. Consequently, magnetite nanoparticles loaded polymeric biomaterials are promising tools for scaffold mediated construction of three-dimensional engineered tissues composed of magnetic controlled orientation of cells and ECM.

* email: zaharia.catalin@gmail.com; Phone: +40 21 4022715

The paper is focused on designing a novel silk fibroin-magnetite biomaterial scaffold for wounds healing in terms of: synthesis, physico-chemical and morphological characterization and *in vitro* biological behaviour assessment

Experimental part

Materials and methods

Cocoons of *Bombyx mori* silkworm silk were kindly supplied by Commercial Society SERICAROM SA (Bucharest, Romania). Lithium bromide (LiBr), sodium bicarbonate and sodium dodecyl sulfate (SDS) were provided by Alfa Aesar GmbH&Co KG, Germany and dialysis tubing cellulose membrane from Sigma. All other chemicals (of analytical grade) were supplied from Sigma Aldrich and are used as received. Magnetic nanoparticles of Fe_3O_4 were obtained directly by co-precipitation using ammonia solution. All the cell culture reagents including the MTT reagent and Tox-7 kit were purchased from Sigma-Aldrich Co. (Steinheim, Germany), while the fluorescent labelling reagents were supplied by Invitrogen, Life Technologies (Foster City, CA).

Cell culture model

Human adipose derived stem cells (hASCs) were isolated from subcutaneous adipose tissue during elective liposuction procedures as previously described [24]. All the patients approved in written the enrolment in the study. None of them suffered from diabetes or other severe systemic illness. All the medical procedures were performed in compliance with the Helsinki Declaration, with the approval of the Emergency Hospital for Plastic Surgery and Burns Ethical Committee (reference No. 3076/10.06.2010). hASCs were seeded at an initial density of 1.5 × 10^4 cells/cm^2 on the composites surfaces and cultured at 37 ^{0}C, 80% humidified atmosphere and 5% CO_2.

Preparation of silk fibroin solution

Bombyx mori silkworm cocoons were boiled for 30 min in an aqueous solution of 0.5 % (w/v) $NaHCO_3$ and SDS and then rinsed thoroughly with distilled water to extract the sericin protein. This operation was repeated three times to get the pure silk fibroin. The degummed silk fibroin was dried at 45 °C and atmospheric pressure. The extracted silk fibroin was then dissolved in a 9.3 M LiBr solution at 65 °C for 12 h, yielding a 8 % (w/v) solution. This solution was dialyzed in distilled water using a dialysis tubing cellulose membrane (molecular weight cut-off, MWCO, 12.4 kDa) for 4 days (frequent water changes). The final concentration of the silk fibroin aqueous solution was 3 wt. %, which was determined by weighing the remaining solid after drying.

Preparation of silk-fibroin magnetite scaffolds (SF-MNP)

The clear silk fibroin solution 3 wt. % was provided. Magnetic nanoparticles (MNP) were dispersed in silk fibroin solution by ultrasonication for several hours. The dispersion of magnetite in silk fibroin solution was cast onto glass dishes followed by solvent evaporation for 48 h. The as obtained membranes were also subjected to drying under vacuum for 24 h. SF-magnetite membranes were obtained with 0.2, 0.3 and 0.45% magnetite content.

FTIR-ATR characterization

Fourier transform infrared (FT-IR) spectra were recorded on a Bruker VERTEX 70 spectrometer in 4000 – 600 cm^{-1} region. The samples were analyzed by attenuated transmission reflectance (ATR).

X-ray diffraction (XRD) spectra were registered on a Panalytical X'PERT MPD X-ray Diffractometer, in the range 2θ= 10–80. An X-ray beam characteristic to Cu Kα radiation was used (λ= 1.5418 Å).

Atomic force microscopy is a powerful modern technique involved in morphological characterization of the material and phase distribution of the multi-component material systems. Morphology investigation was performed by a multimodal Atomic Force Microscope (AFM) in contact mode (Agilent 5500). The apparatus is equipped with a controller AC Mode III A scanner with a scanning capability of 90 μm x 90 μm in the direction xy to 7 μm in the z direction. This is a powerful technique of morphological analysis, which provides a profile of 3D nanoscale surfaces by measuring forces between a sharp tip and the sample surface at very small distances.

Geometrical evaluation (size and shape), crystalline structure of magnetic nanoparticles and the morphology of the scaffolds were investigated by high-resolution transmission electron microscopy (HR-TEM) using a TECNAI F30 G^2 S-TWIN microscope operated at 300 kV with Energy Dispersive X-ray Analysis (EDAX) facility.

Biocompatibility assessment

Live/Dead Fluorescence Microscopy Assay

Cell viability on the novel composites materials was evaluated at 48h post seeding by using fluorescence microscopy Live/Dead assay. In this view, both live and dead cells were simultaneously stained with calcein AM (a non-fluorescent and permeable reagent, which is converted by the intracellular esterases to the intensely green fluorescent calcein - ex/em: ~495 nm/~515 nm) and with ethidium bromide (a dye which enters only the cells with damaged membrane, producing a bright red fluorescence when binding to nucleic acids (ex/em: ~495 nm/~635 nm). Consequently, at 48h post seeding, the hADSCs-composite bioconstructs were incubated with the staining solution prepared according to the manufacturer's instructions for 15 min at room temperature and dark. Next, the stained samples were inspected by fluorescence microscopy using an Olympus IX71 inverted microscope, and images were captured with Cell F Imaging Software (Olympus: Hamburg, Germany, 2008).

MTT Spectrophotometric Test

Cell viability in contact with the composites materials was additionally quantified by MTT spectrophotometric assay at 48h post seeding. This method is based on the reduction of the tetrazolium salt solution (MTT) to purple formazan by metabolically active cells. After 48h of culture, all the samples were incubated at 37^{0}C for 4 h in 1 mg/mL MTT solution. The concentration of the formazan produced by the metabolically active cells was spectrophotometrically quantified at 550 nm (Appliskan Thermo Scientific, Waltham, MA, USA), after solubilisation in isopropanol.

LDH Spectrophotometric Assay

The cytotoxic potential the novel composite materials on hASCs was evaluated using *In vitro toxicology assay kit lactate dehydrogenase based – Tox-7*. Lactate dehydrogenase (LDH) is a cytosolic enzyme and its detection in the culture media is correlated with membrane damage and environmental cytotoxicity. Consequently, the lactate dehydrogenase (LDH) enzymatic activity was quantified in the samples culture medium after 48h post seeding. Briefly, the culture media were harvested and mixed with the solutions provided in the kit, following instructions. After 20 min of incubation the LDH enzymatic

activity was determined by measuring the optic density of the resulting solutions at 490 nm (Appliskan Thermo Scientific).

Statistical Analysis

The statistical evaluation of the data was done using the one-way ANOVA method followed by Bonferroni's multiple comparison test. All experiments were performed in triplicate, and the results were expressed as a mean ± standard deviation (SD) using GraphPad Prism Software (version 3.03; GraphPad Software Inc., San Diego, CA, USA, 2002) for Windows. Differences between samples were considered statistically significant for $p < 0.05$ and highly significant for $p < 0.001$.

Results and discussions

FTIR-ATR analysis

The results of the FTIR-ATR spectra gave us the specific absorbance wavelengths of the specific bonds which appeared in the silk fibroin/magnetite materials, confirming the structure of the new materials (fig. 1). Typical peaks of silk fibroin are 1625, 1513 and 1238 cm^{-1}, characteristic for amide I (C=O stretching), amide II (NH deformation and C–N stretching) and amide III (C–N stretching and N–H deformation). The FTIR analysis of the silk fibroin/magnetite films confirmed the spectral modification. As expected, the presence of magnetite is associated with a shifting towards left of the signals from 1625 to 1650 cm^{-1}, 1513 to 1535 cm^{-1}. The characteristic peak for OH and NH groups becomes broader with the presence of the magnetite in the material.

This shifting of the amides is characteristic for β-sheet structure of silk fibroin within the composite films.

XRD analysis

XRD-diffraction was also employed to check the presence of magnetite in the silk fibroin matrix and to investigate the crystalline structure of the biomaterials (fig. 2).

The XRD pattern of the pure magnetite presents the peaks at $2\theta = 30.27°$, 35.7°, 43.44° and 57.14°, which are indexed to (220), (311), (400) and (511) for Fe_3O_4 (magnetite with face-centered cubic system). Diffractograms of SF-MNP films reveal similar maxima to magnetite, especially at 35.7°((311) index for magnetite) slightly shifted according to nanocomposite composition. Pure SF protein has a specific maxima at around 20 °.

AFM/TEM morphological investigation

The nanostructural characteristics of the composite films and the presence of magnetic nanoparticles within the silk fibroin films were revealed by TEM/HRTEM and AFM investigations. The study of the magnetic silk fibroin membranes through transmission electron microscopy gives information about nanostructure, localization and dispersion of magnetic nanoparticles within the silk fibroin matrix. This study shows that SF scaffolds contain both individually dispersed and cluster-type magnetic nanaoparticles. Figures 3-4 reveal the nanostructure of the SF-MNP 0.2% and SF-MNP 0.45% film. The presence of magnetite onto the surface or within the silk fibroin can be noticed.

AFM investigation shows also the presence and the relative uniform distribution of magnetic nanoparticles onto the surface and within the polymeric matrix in a nice 2D/3D images (deflection and three-dimensional pictures).

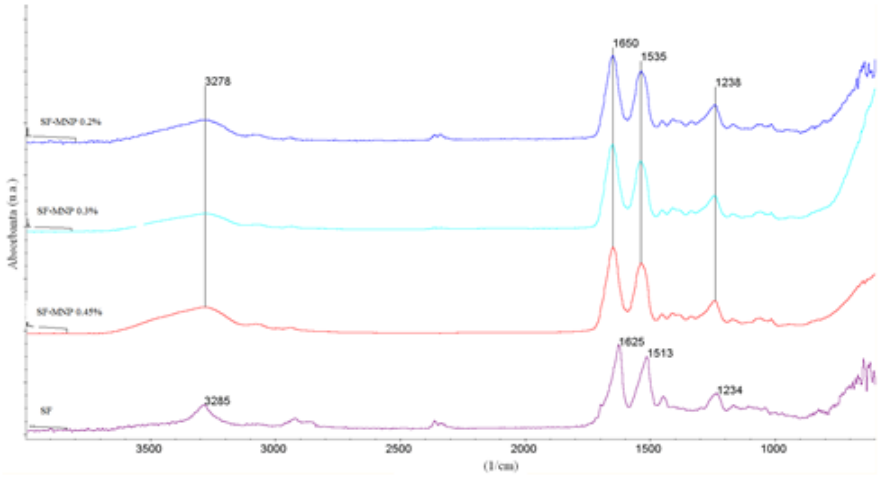

Fig.1. FTIR-ATR spectra of SF and SF-MNP scaffolds

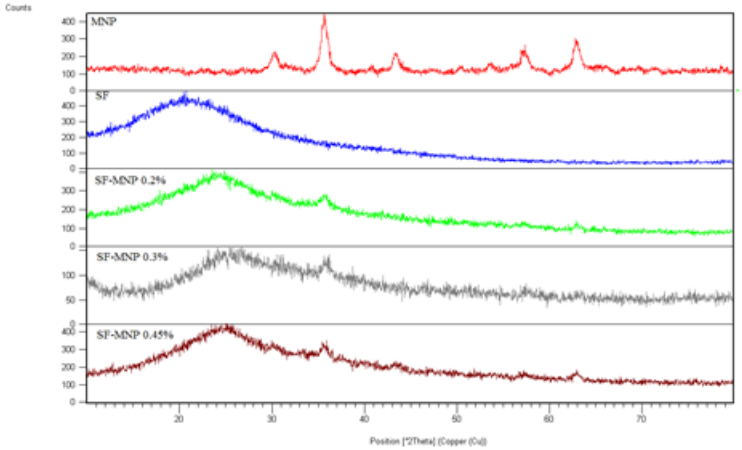

Fig.2. XRD diffractograms of magnetite, SF and SF-MNP scaffolds

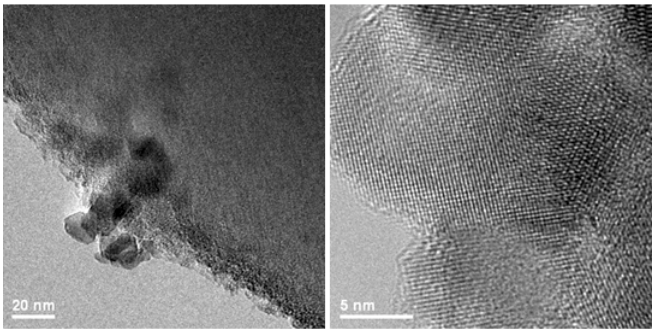

Fig.3. TEM/HRTEM microphotographs of SF-MNP 0.2% scaffolds

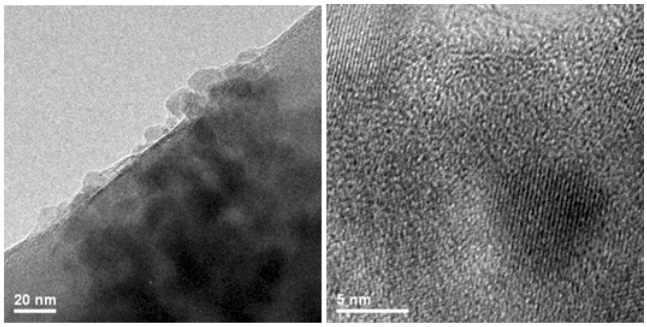

Fig.4. TEM/HRTEM microphotographs of SF-MNP 0.45% scaffolds

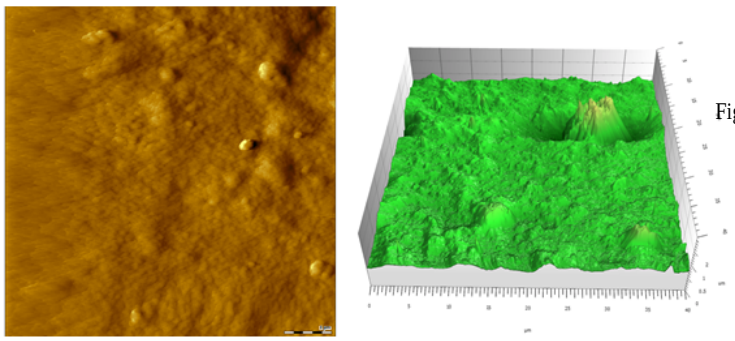
Fig.5. AFM images for silk fibroin-MNP 0.45% scaffolds (deflection and 3D images)

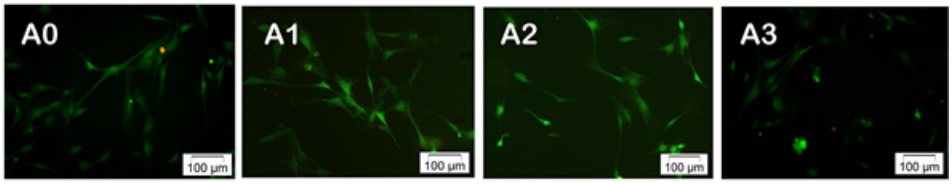

Fig.6. Fluorescence microscopy micrographs revealing live and dead cells on FN (A0), SF-MNP 0.2 % (A1), SF-MNP 0.3 % (A2), SF-MNP 0.45 % (A3) at 48 hours post-seeding

Biological assay

LIVE/DEAD fluorescent microscopy assay

After 48 h post-seeding, live, bright green-labeled cells, were observed on the surface of A0 (crude SF film), A1, A2 and A3 scaffold (SF-MNP 0.2, 0.3 and 0.45 %), as a proof of their survival. As shown in fig. 6, bright green living hASCs on the surface of all biomaterials display their characteristic spindle-*like* morphology.

Additionally, the highest cell density was observed on silk fibroin A0 film, while the amount of green living cells on A1, A2 and A3 was found approximatively equal, but lower than A0.

Quantification of the cellular viability

The spectrophotometric data obtained after investigating cell viability on A0-3 were graphically represented in figure 7. Our data revealed that after 48h of culture hASCs survived in direct contact with the tested biomaterials. No significant differences were detected, neither between the samples and the fibroin film, nor the three compositions of fibroin and magnetite.

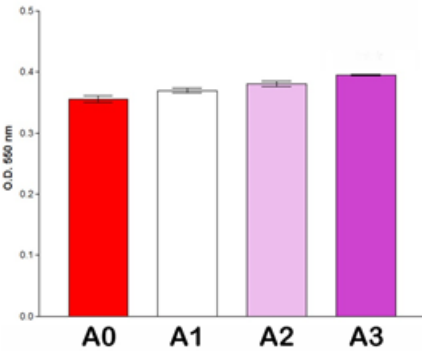

Fig.7. Quantification of hASCs viability on A0, A1, A2 and A3 surfaces, as revealed by MTT test at 48 hours post-seeding

Quantification of the biomaterials cytotoxic potential on hASCs

The cytotoxic potential of A0, A1, A2 and A3 biomaterials was evaluated after 48h of hASCs culture. The spectrophotometric data obtained after LDH enzymatic activity quantification in culture media were represented graphically in figure 8.

Our data did not reveal any statistical significant differences in terms of cytotoxicity between the tested samples.

These results suggest that all the tested magnetic biocomposites display a good biocompatibility *in vitro* on hASCs.

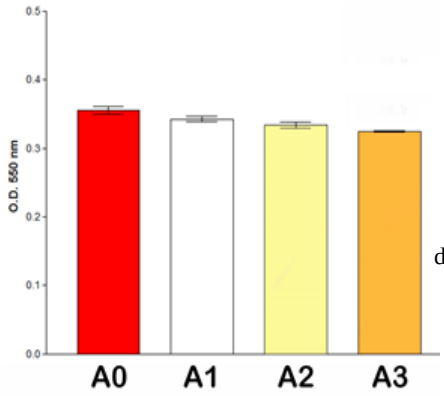

Fig.8. Quantification of LDH enzymatic activity in culture media after 48h of hASCs culture in direct contact with A0, A1, A2 and A3.

Conclusions

Scaffolds based on silk fibroin and magnetic nanoparticles were developed in this study by dispersion of magnetite in silk fibroin solution followed by solvent casting. Physico-chemical and morphological characterization was employed for magnetic silk fibroin biomaterials. The biological assessment show good biocompatibility of the composite films on human adipose derived stem cells (hASCs). These biocomposite materials could be further tested for wound healing applications as

they show promising results in this field of tissue engineering applications.

Acknowledgements: This work was supported by a grant of the Romanian National Authority for Scientific Research and Innovation, CNCS – UEFISCDI, project number PN-II-RU-TE-2014-4-1272, 3/ 01.10.2015.

References

1. MONDAL, M., TRIVEDY, K., KUMAR, S.N., Caspian J. Env. Sci., 5(2), 2007, p. 63.
2. LIN, F., LI, Y., JIN, J., CAI, Y., WEI, K., YAO, J., Materials Chemistry and Physics, 111, 2008, p. 92.
3. ALTMAN, G.H., DIAZ, F., JAKUBA, C., CALABRO, T., HORAN, R.L., CHEN, J., LU, H., RICHMOND, J., KAPLAN, D.L., Biomaterials, 24, 2003, p. 401.
4. CAO, Y., WANG, B., International Journal of Molecular Sciences, 10, 2009, p. 1514.
5. SAH, M.K., PRAMANIK, K., International Journal of Environmental Science and Development, 1(5), 2010, p. 404.
6. MANDAL, B.B., KUNDU, S.C., Acta Biomaterialia, 6, 2010, p. 360.
7. ACHARYA, C., HOSH, S.K., KUNDU, S.C., Acta Biomaterialia, 5, 2009, p. 429.
8. MINOURA, N., AIBA, S.I., HIGUCHI, M., GOTOH, Y., TSUKADA, M., IMAI, Y., Biochemical and Biophysical research communications, 208, 1995, p. 511.
9. ALTMAN, G.H., HORAN, R.L., LU, H.H., MOREAU, J., MARTIN, I., RICHMOND, J.C., KAPLAN, D.L., Biomaterials, 23, 2002, p. 4131.
10. LEAL-EGANA, A., SCHEIBEL, T., Biotechnol. Appl. Biochem., 55, 2010, p. 155.
11. ZHANG, Q., YAN, S., LI, M., Materials, 2, 2009, pp. 2276.
12. KASOJU, N., BORA, U., Adv. Healthcare Mater., 1, 2012, p. 393.
13. SASHINA, E.S., BOCHEK, A.M., NOVOSELOV, N.P., KIRICHENKO, D.A., Russian Journal of Applied Chemistry, 79(6), 2006, p. 869.
14. ZAHARIA, C., TUDORA, M.R., STANCU, I.C., GALATEANU, B., LUNGU, A., CINCU, C., Materials Science And Engineering C, 32, 2012, p. 945.
15. XIAO, W., HE, J., NICHOL, J.W., WANG, L., HUTSON, C.B., WANG, B., et al., Acta Biomaterialia, 7, 2011, p. 2384.
16 ETIENNE, O., SCHNEIDER, A., KLUGE, J.A., BELLEMIN-LAPONNAZ, C., POLIDORI, C., LEISK, G.G., et al., Journal of Periodontology, 80 2009, p. 1852.
17. LOVETT, M., CANNIZZARO, C., DAHERON, L., MESSMER, B., VUNJAK-NOVAKOVIC, G., KAPLAN, D.L., Biomaterials, 28, 2007, p. 5271.
18. SRIHANAM, P., Biotechnology, 10, 2011, p. 114.
19. LACOEUILLE, F., HINDRE, F., VENIER-JULIENNE, M.C., SERGENT, M., BOUCHET, F., JOUANETON, M.S., et al., Biomaterials, 32, 2011, p. 7999.
20. INUKAI, A., SAKAMOTO, N., AONO, H., SAKURAI, O., SHINOZAKI, K., SUZUKI, H., WAKIYA, N., Journal of Magnetism and Magnetic Materials, 323(7), 2011, p. 965.
21. GHAEMY, M., NASERI, M., Carbohydrate Polymers, 90(3), 2012, p. 1265.
22.AJEESH, M., FRANCIS, B., ANNIE, J., VARMA, P.H., Journal of Materials Science, Materials in Medicine, 21(5), 2010, p. 1427.
23. KUDA, O., PINCHUK, N., IVANCHENKO, L., PARKHOMEY, O., SYCH, O., LEONOWICZ, M., WROBLEWSKI, R., SOWKA, E., Journal of Materials Processing Technology, 209(4), 2009, p. 1960.
24. GALATEANU, B., DINESCU, S., CIMPEAN, A., DINISCHIOTU, A., COSTACHE, M., Int. J. Mol. Sci., 13, 2012, p.15881 (doi:10.3390/ ijms131215881)

Manuscript received: 10.11.2016